

11-7-2021

Electronic structure and estimation of Curie temperature in Ca_2BIrO_6 (B = Cr, Fe) double perovskites

Shalika Ram Bhandari
Tribhuvan University

Santosh KC
San Jose State University, santosh.kc@sjsu.edu

Sarita Lawaju
Tribhuvan University

Ram Kumar Thapa
Mizoram University

Gopi Chandra Kaphle
Tribhuvan University

See next page for additional authors

Follow this and additional works at: https://scholarworks.sjsu.edu/faculty_rsca

Recommended Citation

Shalika Ram Bhandari, Santosh KC, Sarita Lawaju, Ram Kumar Thapa, Gopi Chandra Kaphle, and Madhav Prasad Ghimire. "Electronic structure and estimation of Curie temperature in Ca_2BIrO_6 (B = Cr, Fe) double perovskites" *Journal of Applied Physics* (2021). <https://doi.org/10.1063/5.0069884>

This Article is brought to you for free and open access by SJSU ScholarWorks. It has been accepted for inclusion in Faculty Research, Scholarly, and Creative Activity by an authorized administrator of SJSU ScholarWorks. For more information, please contact scholarworks@sjsu.edu.

Authors

Shalika Ram Bhandari, Santosh KC, Sarita Lawaju, Ram Kumar Thapa, Gopi Chandra Kaphle, and Madhav Prasad Ghimire

RESEARCH ARTICLE | NOVEMBER 02 2021

Electronic structure and estimation of Curie temperature in Ca_2BIrO_6 (B = Cr, Fe) double perovskites

Shalika Ram Bhandari; Santosh KC; Sarita Lawaju; ... et. al



Journal of Applied Physics 130, 173902 (2021)

<https://doi.org/10.1063/5.0069884>



CrossMark

Articles You May Be Interested In

Near compensated half-metal in $\text{Sr}_2\text{NiOsO}_6$

J. Chem. Phys. (March 2009)

Effect of alkaline-earth and transition metals on the electrical transport of double perovskites

Journal of Applied Physics (May 2004)

Time to get excited.
Lock-in Amplifiers – from DC to 8.5 GHz

Find out more

Zurich Instruments






Electronic structure and estimation of Curie temperature in $\text{Ca}_2\text{BIR}_2\text{O}_6$ (B = Cr, Fe) double perovskites

Cite as: J. Appl. Phys. **130**, 173902 (2021); doi: [10.1063/5.0069884](https://doi.org/10.1063/5.0069884)

Submitted: 2 September 2021 · Accepted: 14 October 2021 ·

Published Online: 2 November 2021



Shalika Ram Bhandari,^{1,2,3}  Santosh KC,⁴  Sarita Lawaju,¹  Ram Kumar Thapa,⁵  Gopi Chandra Kaphle,¹ 
and Madhav Prasad Ghimire^{1,2,3,a)} 

AFFILIATIONS

¹Central Department of Physics, Tribhuvan University, Kirtipur, Bagmati 44613, Nepal

²Leibniz Institute for Solid State and Materials Research Dresden (IFW-Dresden), Dresden 01609, Germany

³Condensed Matter Physics Research Center, Butwal-11, Lumbini 32907, Nepal

⁴Chemical and Materials Engineering, San José State University, San Jose, California 95192, USA

⁵Department of Physics, Mizoram University, Aizawl, Mizoram 796004, India

^{a)}Author to whom correspondence should be addressed: madhav.ghimire@cdp.tu.edu.np

ABSTRACT

We investigate the electronic and magnetic properties of $\text{Ca}_2\text{CrIrO}_6$ and $\text{Ca}_2\text{FeIrO}_6$ by means of density functional theory. These materials belong to a family of recently synthesized $\text{Ca}_2\text{CrOsO}_6$ whose properties show possible applications in a room temperature regime. Upon replacement of Os by Ir in $\text{Ca}_2\text{CrOsO}_6$, we found the system to exhibit a stable ferrimagnetic configuration with a bandgap of ~ 0.25 eV and an effective magnetic moment of $\sim 2.58\mu_B$ per unit cell. Furthermore, when chemical doping is considered by replacing Cr with Fe and Os with Ir, the material retains the insulating state but with a reduced bandgap of 0.13 eV and large increment in the effective magnetic moment of $\sim 6.68\mu_B$ per unit cell. These observed behaviors are noted to be the consequence of the cooperative effect of spin-orbit coupling; Coulomb correlations from Cr-3d, Fe-3d, and Ir-5d electrons; and the crystal field effect of the materials. These calculations suggest that by chemical tuning, one can manipulate the bandgap and their effective magnetic moment, which may help in material fabrication for device applications. To check further the suitability and applicability of $\text{Ca}_2\text{CrIrO}_6$ and $\text{Ca}_2\text{FeIrO}_6$ at higher temperatures, we estimate the Curie temperature (T_C) by calculating the spin-exchange coupling. We found that our findings are in a valid T_C trend similar to other perovskites. Our findings are expected to be useful in experimental synthesis and transport measurement for potential applications in modern technological devices.

Published under an exclusive license by AIP Publishing. <https://doi.org/10.1063/5.0069884>

I. INTRODUCTION

Double perovskites (DPs), derived from the general formula $\text{A}_2\text{BB}'\text{O}_6$ [where B and B' cations are transition metals (TMs) and A and A' sites are alkaline or rare earth metals], are found to have various properties with potential applications. Transition metal (TM)-based DPs are of interest due to their remarkable properties including structural stability, high charge mobility, finite bandgap, superconductivity, half-metallicity, piezo-electricity, thermo-electricity, topological properties, etc. These peculiar properties are important to integrate with modern technological devices.¹⁻⁹ Recently, various DP materials have been reported with different

novel properties, such as antiferromagnetism (AFM) in SrLaNiIrO_6 , weak paramagnetism (PM) in SrLaMgIrO_6 ,¹⁰ ferromagnetism in Ba_2NiUO_6 ,¹¹ magnetic insulating state in $\text{Sr}_2\text{CuOsO}_6$ and $\text{Sr}_2\text{NiOsO}_6$,¹² half-semi-metallic AFM in $\text{Sr}_2\text{CrOsO}_6$ (SCOO) and $\text{Sr}_2\text{CrRuO}_6$,¹³ ferrimagnetism with high Curie temperature in $\text{Sr}_2\text{CrIrO}_6$ (SCIO),¹⁴ Dirac insulating ferromagnetic (FM) state near 100 K,¹⁵ and quantum anomalous Hall (QAH) effect in $\text{Ba}_2\text{NiOsO}_6$.¹⁶ The A-site occupied with a transition metal in DP $\text{Mn}_2\text{FeReO}_6$ shows half-metallic ferrimagnetism with a transition temperature of 520 K above room temperature with a positive magnetoresistance behavior.¹⁷ In a few cases, Coulomb correlation is

sufficient to explore the Mott insulating state in AFM systems such as $\text{Ca}_2\text{MgOsO}_6$ and $\text{Sr}_2\text{MgOsO}_6$.¹⁸ Based on density functional theory (DFT) calculations, it was reported that the Mott insulating state of $\text{Sr}_2\text{NiOsO}_6$, $\text{Sr}_2\text{FeOsO}_6$, and $\text{Sr}_2\text{NiRuO}_6$ arises as a result of electron-correlation and spin-orbit coupling (SOC).¹⁹ A study by Monte Carlo simulations on Sr_2VMoO_6 shows the dependency of blocking temperature, magnetic properties on the crystal field, the system size, and the coupling constants, and on $\text{Lu}_2\text{MnCoO}_6$, phase transitions and the magnetic stability along with exchange coupling were calculated.^{20,21}

In addition, the correlated-metal oxides, in particular, iridates and rhodates, lead to unconventional phases.^{22,23} Among them, iridate-based materials that yield various unconventional phases in cooperation with strongly correlated effects due to the strong Coulomb interaction among electrons have shown interesting features. For example, Sr_2IrO_4 ^{24,25} is reported as a Mott insulator, $\text{Ln}_2\text{Ir}_2\text{O}_7$ ²² is a topological Mott insulator, $\text{Y}_2\text{Ir}_2\text{O}_7$ ²⁶ is a topological semimetal with a Fermi-arc on the surface, $\text{Pr}_2\text{MgIrO}_6$ ²⁷ is a ferrimagnetic (FIM) Mott-Hubbard insulator, $\text{Bi}_2\text{FeIrO}_6$ ²⁸ is an FM insulator, and PrSrMgIrO_6 shows half-metallic AFM (HMAFM) with zero effective moment per unit cell.²⁹ A second-order transition and ferrimagnetism have been reported on $\text{Sr}_2\text{RuHoO}_6$ ³⁰ with the mean-field approximation (MFA) and Monte Carlo calculations.

Here, we report $\text{Ca}_2\text{CrIrO}_6$ (CCIO) and $\text{Ca}_2\text{FeIrO}_6$ (CFIO), which have no experimental or theoretical information on the magnetic transition temperature yet. For investigating the electronic and magnetic transition temperatures, we take $\text{Ca}_2\text{CrOsO}_6$ (CCOO) as a reference material, which is found to be an FIM insulator with a large Curie temperature (T_C) of 490 K.³¹ The reference material $\text{Ca}_2\text{CrOsO}_6$ was reported by some of us as an FIM insulator with a total magnetic moment $\mu_{\text{tot}} = 0.21\mu_B$ per unit cell.³² In this work, we propose $\text{Ca}_2\text{CrIrO}_6$ and $\text{Ca}_2\text{FeIrO}_6$, obtained by substituting Fe in place of Cr and Ir in place of Os, as new FIM insulators in the family of $\text{Ca}_2\text{BB}'\text{O}_6$. The materials are expected to be

suitable for spintronic device applications. To our knowledge and survey, there is no report yet on these new materials. The main motivation to explore $\text{Ca}_2\text{CrIrO}_6$ and $\text{Ca}_2\text{FeIrO}_6$ was to obtain (i) high transition temperature (T_C) above room temperature, (ii) FIM insulating ground state, and (iii) small effective moment. With electron doping, the material is expected to show new properties with rise in T_C . The associated features are expected to be important in new DP-based spintronic devices that work at room temperature. With this report, we expect that new materials can be synthesized experimentally based on this result. Here, we report the structural, electronic, and magnetic properties on the basis of DFT calculations. Section II presents the computational methods, while results and discussion are presented in Sec. III. Finally, conclusions of the research are provided in Sec. IV.

II. COMPUTATIONAL METHOD

To investigate the electronic and magnetic properties^{38,39} of the proposed materials, DFT calculations were performed with the full-potential linearized augmented plane wave method as implemented in WIEN2k code³⁵ and the all-electron full-potential local-orbital (FPLO)^{36,37} code using the standard generalized gradient approximation (GGA) of Perdew-Burke-Ernzerhof (PBE).⁴⁰ To incorporate the correlation effects, Coulomb interaction U is 4 eV for Cr, 5 eV for Fe, and 1.5 eV for Ir.^{41,42} The magnetic anisotropy energy (MAE) was calculated by a self-consistent full-relativistic mode. A set of 500 k -points was used within the full Brillouin zone, which produces a set of $8 \times 8 \times 6$ k -mesh. To consider different magnetic configurations, the monoclinic structure (space group 14) was split to lower symmetry (space group $2:P\bar{1}$) that corresponds to 20 inequivalent atoms.

III. RESULTS AND DISCUSSION

The crystal structure of $\text{Ca}_2\text{BIRoO}_6$ shown in Fig. 1 falls in the space group $P2_1/n$ with monoclinic structure maintained by BO_6 (where B = Cr, Fe) and IrO_6 octahedra. The experimental lattice

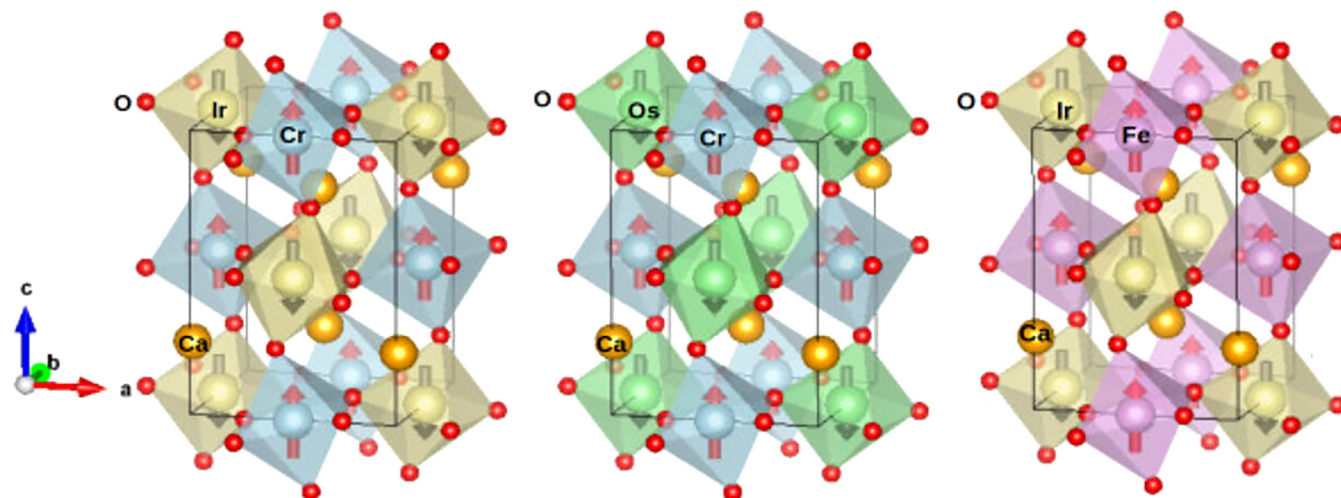


FIG. 1. Crystal structure of $\text{Ca}_2\text{BIRoO}_6$ (gray, purple, sky blue, green, maroon, and red spheres correspond to Ca, Cr, Ir, Os, Fe, and O atoms, respectively).

parameters opted for the calculations are $a = 5.351 \text{ \AA}$, $b = 5.456 \text{ \AA}$, and $c = 7.620 \text{ \AA}$. On the basis of adaptation of the Goldschmidt tolerance factor $t = (r_A + r_O)/\sqrt{2}((r_B/2) + (r'_B/2) + r_O)$,³³ where r_A , r_B , and r'_B are the ionic radii of the respective ions and r_O is the ionic radius of oxygen, we select Fe and Ir elements for substitutions to obtain $\text{Ca}_2\text{CrIrO}_6$ and $\text{Ca}_2\text{FeIrO}_6$ structure, respectively. For the DP family, it is well known that if $t < 0.97$, the compound is either monoclinic or orthorhombic.³⁴

To check the stability of the substituted compounds, the cohesive and formation energies for both the compounds are calculated,

$$E_{\text{For}} = E_{\text{Ca}_2\text{BIR}_6}^{\text{Tot}} - [2E_{\text{Ca}}^{\text{bulk}} + E_{\text{B}}^{\text{bulk}} + E_{\text{Ir}}^{\text{bulk}} + 6E_{\text{O}}^{\text{bulk}}] \quad (1)$$

and

$$E_{\text{Coh}} = E_{\text{Ca}_2\text{BIR}_6}^{\text{Tot}} - [2E_{\text{Ca}}^{\text{iso}} + E_{\text{B}}^{\text{iso}} + E_{\text{Ir}}^{\text{iso}} + 6E_{\text{O}}^{\text{iso}}], \quad (2)$$

where $\text{B} = \text{Cr, Fe}$; $E_{\text{Ca}_2\text{BIR}_6}^{\text{Tot}}$ is the total energy obtained from DFT for Ca_2BIR_6 ; $E_{\text{Ca}}^{\text{bulk}}$, $E_{\text{B}}^{\text{bulk}}$, $E_{\text{Ir}}^{\text{bulk}}$, and $E_{\text{O}}^{\text{bulk}}$ are energies of the bulk of Ca, B, Ir, and O elements; and $E_{\text{Ca}}^{\text{iso}}$, $E_{\text{B}}^{\text{iso}}$, $E_{\text{Ir}}^{\text{iso}}$, and $E_{\text{O}}^{\text{iso}}$ are energies of isolated Ca, B, Ir, and O elements, respectively. The formation and cohesive energies per atom for the materials $\text{Ca}_2\text{CrIrO}_6$ and $\text{Ca}_2\text{FeIrO}_6$ are found to be -2.84 , -2.66 , -4.54 , and -4.25 eV, respectively. The negative values for both cohesive and formation energies confirm that both the materials have a thermodynamically stable structure and are possible to synthesize experimentally.

We then analyze the electronic and magnetic properties of DP. We begin our discussion starting from the magnetic ground state. For this, we first optimize the internal parameters and have

considered five types of magnetic configurations: one FM ($\text{FM1-}\uparrow\uparrow\uparrow\uparrow$), two AFM ($\text{AF1-}\uparrow\downarrow\uparrow\downarrow$, $\text{AF2-}\uparrow\downarrow\downarrow\uparrow$), and two FIM ($\text{FIM1-}\uparrow\uparrow\downarrow\downarrow$, $\text{FIM2-}\uparrow\uparrow\uparrow\downarrow$), respectively, for both the systems with an energy difference of 159 and 80 meV between FIM1 and first excited FM structure for $\text{Ca}_2\text{CrIrO}_6$ and $\text{Ca}_2\text{FeIrO}_6$, respectively. FIM1 is found to have the lowest energy for both the materials indicating the magnetic ground state with a magnetic easy axis along the [010] direction for $\text{Ca}_2\text{CrIrO}_6$ and along the [100] direction for $\text{Ca}_2\text{FeIrO}_6$, and MAE is found to be 8 and 12 meV, respectively.

In $\text{Ca}_2\text{CrIrO}_6$, within GGA, the TM Cr takes the charge state the +3 with $3d^3$ configuration and is coupled ferrimagnetically with Ir. The three d electrons of Cr go to t_{2g} states for the spin-up channel and hence remain in the valence region, while for the spin-down channel, they remain in the conduction region and the e_g state remains empty for both channels so it lies in the conduction region. For Ir, it takes charge state +5 with the d^4 configuration where three electrons go to the spin-down channel in the t_{2g} state and hence remain close to the Fermi level (E_F) in the valence region and one remaining electron goes to the t_{2g} state with spin-up forming a low spin state as seen in Fig. 2.

Likewise, in $\text{Ca}_2\text{FeIrO}_6$, Fe has five outer most electrons with a $3d^5$ configuration and has a charge state +3 and is found to be occupied in the spin-up channel and empty in the spin-down channel. Hence, the density of states (DOS) lies deep in the valence region while states in the spin-down channel lie far in the conduction region giving rise to the high spin state of Fe. In the case of Ir, it has a $5d^4$ configuration with the charge state +5. The three outermost electrons reside for the spin-down channel and hence they remain in the upper most valence region just below the Fermi level (E_F) and one remaining electron goes to the t_{2g} state giving a low

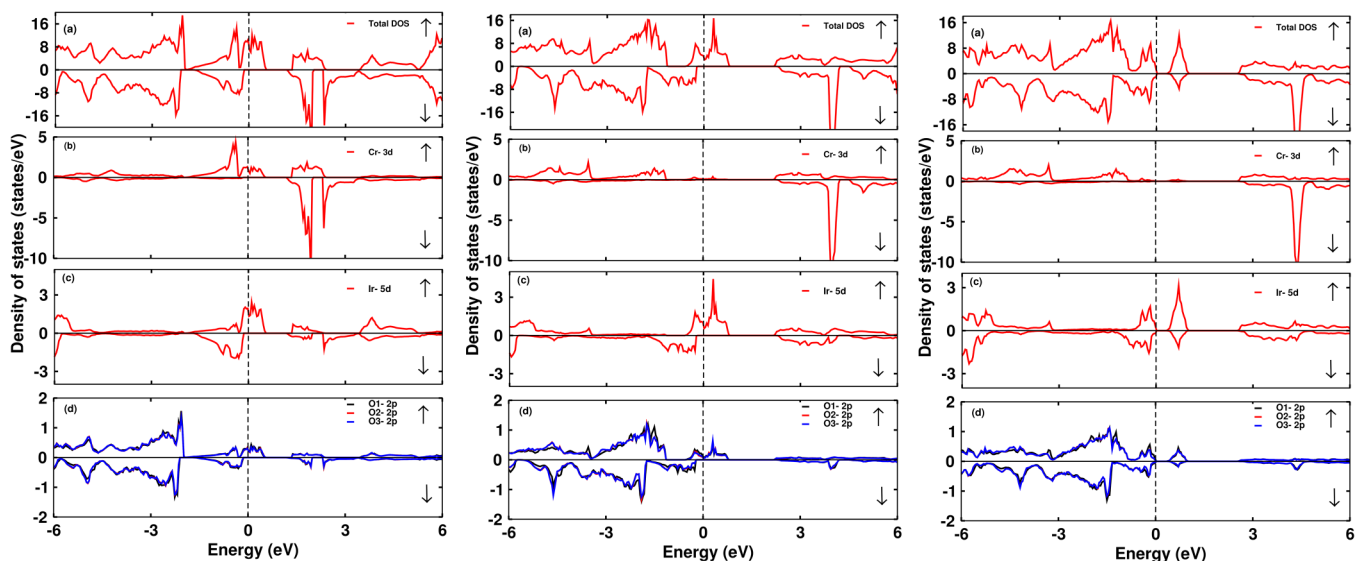


FIG. 2. The total and partial density of states (PDOS) of $\text{Ca}_2\text{CrIrO}_6$ within GGA (left), GGA + U (middle) and GGA + U + SOC functional (right), respectively. (a) Total density of states (DOS), (b) partial DOS of Cr-3d, (c) PDOS of Ir-5d, and (d) PDOS of O-2p atoms for spin-up (\uparrow) and spin-down (\downarrow) for $\text{Ca}_2\text{CrIrO}_6$. The vertical dotted line indicates $E_F = 0$.

spin state as in Fig. 3. Two unoccupied t_{2g} states are found in the conduction region represented by a peak for the spin-up channel.

The presence of $3d$ elements in the material is supposed to have a strong correlation effect, which was ignored in the calculations within GGA. Here, we extend our calculation with GGA + U taking $U = 4$ eV for Cr, 5 eV for Fe, and 1.5 eV for Ir. Since the strength of the SOC in Ir plays a significant role indicating the electronic properties, we further performed calculations with GGA + U + SOC. As expected, the metallic state transforms to the semiconducting state with bandgaps of 0.25 and 0.13 eV for Cr and Fe, respectively. After SOC, we observe a noticeable change in the Ir- $5d$ bands in which it splits near E_F as observed in DOS and band structures (see Figs. 2–4).

The spin resolved total and partial density of states (PDOS) for $\text{Ca}_2\text{CrIrO}_6$ within GGA, GGA + U , and GGA + U + SOC are shown in Figs. 2 and 3. The major contribution to the total DOS around E_F is mainly from Cr- $3d$, Ir- $5d$, and O- $2p$ states. The Ir- $5d$ states are found to play a key role indicating the electronic properties. They are found to hybridize strongly with the O- $2p$ states in both spin channels. Their hybridization occurs mostly in the valence region near E_F and in the conduction region. We observe that Ir- t_{2g} states are fully occupied in spin-down channels and thus lie in the valence region, whereas in the spin-up channel, the states being empty lie in the conduction region along with other unoccupied Ir- e_g states. This is found to be consistent with the ionic picture of Ir. The charge transfer effect is prominent between Ir- $5d$ and O- $2p$ states due to strong hybridization. This induces sizable moments in oxygen atoms, which get polarized in parallel with Ir atoms.

We further considered the magnetic behavior of Ca_2BIrO_6 . As tabulated in Table I, the calculated magnetic moments for Fe and Ir sites are found to be $4.12\mu_B$ and $-0.73\mu_B$, respectively. The

calculated orbital moment at the Fe site is small, that is, $0.027\mu_B$, and aligns in the same direction as the spin moment, confirming the half-filled $5d^5$ configuration of Fe in $\text{Ca}_2\text{FeIrO}_6$, which is in accordance with Hund's third rule.⁴³ The calculated orbital moment at the Ir site is found to be $-0.26\mu_B$ in a parallel direction with spin magnetic moments contributing to an effective magnetic moment of $6.66\mu_B$ per unit cell.

Moving on to $\text{Ca}_2\text{CrIrO}_6$, the spin and orbital moments for Cr are found to be $2.54\mu_B$ and $-0.1\mu_B$, respectively, and align in the antiparallel direction showing that the $3d$ orbital is either less or more than half filled. From Table I, the spin magnetic moment in Ir is slightly reduced due to the Ir-O hybridization and influence of SOC, whereas in Ir- $5d$, orbital magnetic moments are found to be $-0.28\mu_B$ in the same direction of the orbital magnetic moment of Cr, which increases the net magnetic moment to $2.59\mu_B$.

Due to the partial charge transfer from Cr, Fe, and Ir to oxygen, it also gains a sizeable moment of $0.08\mu_B$ in $\text{Ca}_2\text{CrIrO}_6$ and $0.01\mu_B$ in $\text{Ca}_2\text{FeIrO}_6$, and polarization is mainly on O- $2p$ orbitals consistent with the spin magnetization isosurface plot shown in Fig. 5. Here, the polarization is mainly found in $2p$ orbitals, and this hybridized moment in oxygen increases the resultant moment. Interestingly, the developed magnetic moments at the O site are aligned in the direction of the Ir moment, suggesting a stronger interaction among Ir-O than that of Cr-O in $\text{Ca}_2\text{CrIrO}_6$.

Further to note in Fig. 5 is that the isosurface of Cr- $3d$ states is in a dumb-bell-like shape, which is formed due to the t_{2g} orbitals. The contribution of charge distribution is due to the t_{2g} state, and to Ir, charge distribution is in the spin-down channel in t_{2g} states. Upon replacement of the Cr by Fe atom, both the t_{2g} state and the e_g state are fully occupied in the spin-up channel but remain empty in the spin-down channel. Hence, the contribution

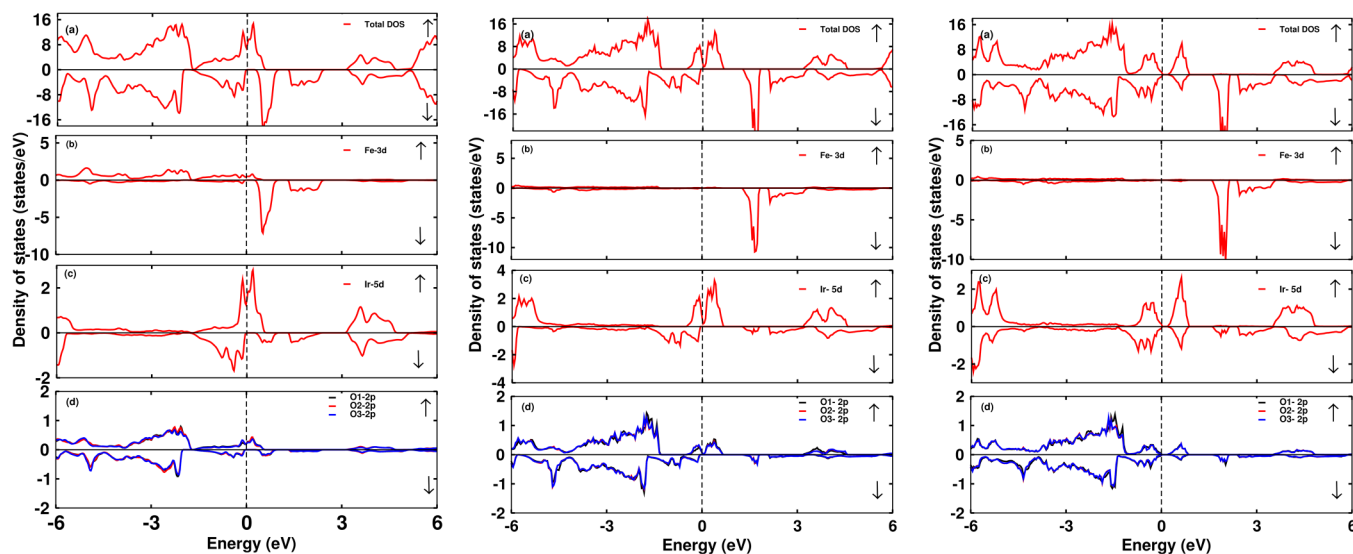


FIG. 3. The total and partial DOS of $\text{Ca}_2\text{FeIrO}_6$ within GGA (left), GGA + U (middle), and GGA + U + SOC functional (right), respectively. (a) Total density of states (DOS), (b) partial DOS of Fe- $3d$, (c) PDOS of Ir- $5d$, and (d) PDOS of O- $2p$ atoms for spin-up (\uparrow) and spin-down (\downarrow) for $\text{Ca}_2\text{FeIrO}_6$. The vertical dotted line indicates $E_F = 0$.

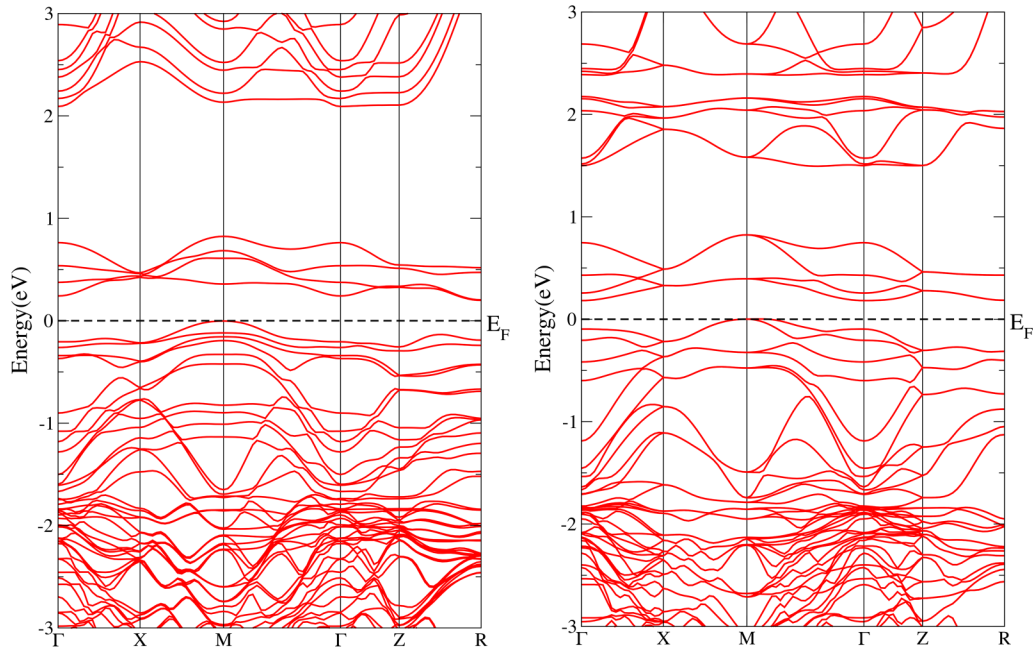


FIG. 4. The band structures of $\text{Ca}_2\text{CrIrO}_6$ (left) and $\text{Ca}_2\text{FeIrO}_6$ (right) within GGA + U + SOC. The horizontal dotted line indicates $E_F = 0$.

to the spin magnetization is by both t_{2g} and e_g states. As a result, the isosurface of Fe is spherical, and Ir contribution remains the same as in Fig. 5 (right).

In order to understand the suitability of the proposed materials, we have computed the spin-exchange coupling parameters by computing the total energy for several collinear spin configurations of Cr, Fe, and Ir and are mapped into the spin model. For the same, we utilize the exchange parameters for estimating the magnetic transition temperature based on the Heisenberg model of mean-field approximation (MFA).

The Hamiltonian for the interaction of spins can be written as

$$\hat{H} = - \sum_{i < j} J_{ij} \hat{S}_i \hat{S}_j, \quad (3)$$

where (J_{ij}) is the exchange coupling constant between spins at sites i and j , where i, j represent the atomic sites in the crystal ($S_{\text{Fe}} = 5/2$, $S_{\text{Cr}} = 3/2$, $S_{\text{Ir}} = 3/2$), as shown in Fig. 6; J_1 is for $J_{\text{Cr-Cr}}$ (in-plane); J_2 is for $J_{\text{Fe-Fe}}$ (in-plane); and J_3 is for $J_{\text{Cr-Fe}}$ (out-of-plane) with nearest neighbors of 6, 12, and 12, respectively, considered for calculations.

The estimated J parameters, description of the atoms, and respective nearest neighbors for DP $\text{Ca}_2\text{CrIrO}_6$ and $\text{Ca}_2\text{FeIrO}_6$ are shown in Table II. Our results are found to be within the limitation with GGA + U calculations, which tends to localize the orbitals decreasing the overlap between magnetic orbitals. As a result, this reduces the spin-exchange interactions and, hence, the estimation of magnetic transition temperature in the materials.

TABLE I. Calculated spin magnetic moments (in μ_B) of B (Cr/Fe), B' (Ir), three oxygen atoms, and bandgap " E_g " (eV). The calculated orbital moments at B and B' sites are shown within parentheses for $\text{Ca}_2\text{BrIrO}_6$ HM denotes the half-metallic state.

Site	$\text{Ca}_2\text{CrIrO}_6$			$\text{Ca}_2\text{FeIrO}_6$		
	GGA	GGA + U	GGA + U + SOC	GGA	GGA + U	GGA + U + SOC
B	2.12	2.55	2.54/−0.073	3.48	4.12	4.12/0.027
B'	−0.72	−0.96	−0.82/−0.284	−0.55	−0.87	−0.728/−0.263
O1	−0.08	−0.10	−0.078	0.0061	−0.038	−0.007
O2	−0.076	−0.11	−0.083	0.015	−0.023	0.003
O3	−0.072	−0.10	−0.085	0.012	−0.025	−0.009
Tot. mom.	2.0	2.0	2.59	6.0	5.99	6.66
E_g	HM	HM	0.25	HM	HM	0.13

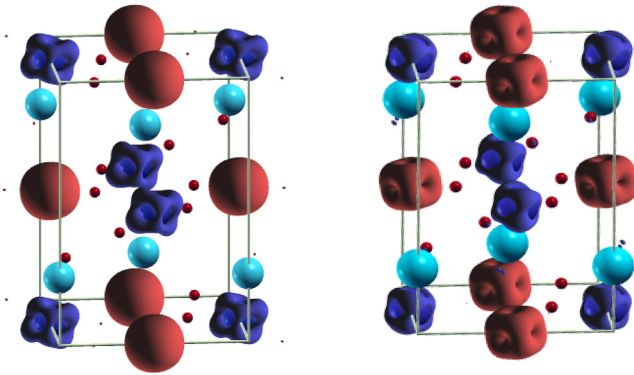


FIG. 5. Isosurface of spin magnetization density at $\pm 0.23e/A^3$ with red (blue) for spin-up (down): left, Ca_2FeIrO_6 ; right, material with Cr replacement Ca_2CrIrO_6 [royal blue, sky blue, maroon, and red colors represent Ir, Ca, Cr (Fe), and O, respectively].

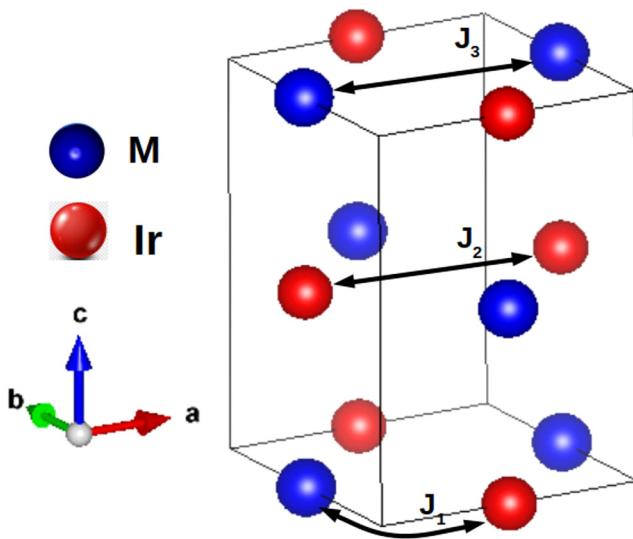


FIG. 6. Computed magnetic exchange interactions in the double perovskite configuration Ca_2CrIrO_6 and Ca_2FeIrO_6 . The atom label M in the figure refers to Cr or Fe.

TABLE II. Estimated magnetic exchange coupling parameters (in meV) for double perovskite Ca_2MlIrO_6 , M = Cr/Fe.

Interaction	Description	Nearest neighbor	Distance	
			M = Cr	M = Fe
J_1	M–Ir	6	–3.21	–3.55
J_2	Ir–Ir	12	–4.25	–0.8
J_3	M–M	12	5.85	–0.32

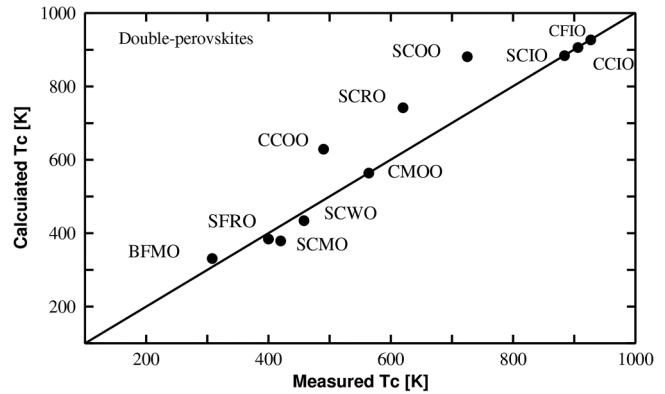


FIG. 7. Calculated vs measured Curie temperatures for different double perovskites.

We have also estimated the Curie temperature of the proposed materials using the mean-field theory as

$$T_C = S_i S_j \frac{2 \sum J_{ij}}{3 K_B}, \quad (4)$$

where S_i and S_j are the spin quantum numbers at i and j sublattices, respectively. Our calculated T_C are found to be 906 and 836 K for Ca_2CrIrO_6 and Ca_2FeIrO_6 , respectively. As shown in Fig. 7, we have compared the measured and calculated Curie temperatures. Different DPs with their respective T_C presented in Fig. 7 are Ba_2FeMoO_6 (BFMO),⁴⁴ Sr_2FeReO_6 (SFRO),⁴⁴ Sr_2CrMoO_6 (SCMO),⁴⁵ Sr_2CrWO_6 (SCWO),⁴⁴ Ca_2CrOsO_6 (CCOO),^{31,46} Ca_2MnOsO_6 (CMOO),⁴⁶ Sr_2CrReO_6 (SCRO),⁴⁷ Sr_2CrOsO_6 (SCOO),⁴⁸ Sr_2CrIrO_6 (SCIO),⁴⁹ Ca_2CrIrO_6 (CCIO), and Ca_2FeIrO_6 (CFIO). By comparing the calculated T_C of the materials with a similar work as reported by Mandal *et al.*,⁴⁹ we found a decent agreement of our result though no experimental report of T_C has been studied on these materials. Our theoretical value of T_C for the studied compounds may be slightly larger than their true values in similar materials. This may happen since the mean-field theory often overestimates the T_C , and the absolute value of T_C depends on the selected U values. Nonetheless, our results are expected to give a valid T_C trend as observed in Fig. 7 for the considered compounds.⁶

IV. CONCLUSIONS

We performed density functional theory to identify the electronic, magnetic, and ordering temperatures of yet to be synthesized materials Ca_2CrIrO_6 and Ca_2FeIrO_6 . We found that they are insulating in nature under the cooperative effect of Coulomb interactions and spin–orbit coupling. The effect is found to be significant in opening the bandgap. The bandgap was noted to be 0.25 eV for Ca_2CrIrO_6 and 0.13 eV for Ca_2FeIrO_6 . Furthermore, we estimated the Curie temperature (T_C) that was found to be 906 and 836 K for Ca_2CrIrO_6 and Ca_2FeIrO_6 , respectively, which are in a valid T_C range as in other similar compounds. Our predicted value is expected to initiate further experimental efforts to verify the interesting predictions made in this work.

Downloaded from http://pubs.aip.org/aip/jap/article-pdf/doi/10.1063/5.0069884/1527196/1.173902_1_online.pdf

ACKNOWLEDGMENTS

S.R.B. acknowledges the Nepal Academy of Science and Technology, Khumaltar, Nepal, for the Ph.D. fellowship. M.P.G. acknowledges the Alexander von Humboldt Foundation, Germany, for the equipment subsidy grants. S.K.C. acknowledges the faculty start-up grant provided by Davidson College of Engineering at San José State University. S.R.B. and M.P.G. are grateful for fruitful discussions with M. Richter and J. van den brink of IFW Dresden. Computations were performed at IFW Dresden, Germany, and Advanced Materials Research Laboratory, Central Department of Physics, Tribhuvan University, Nepal. We are thankful to Ulrike Nitzsche for the technical assistance.

AUTHOR DECLARATIONS

Conflict of Interest

The authors have no conflicts to disclose.

DATA AVAILABILITY

The data that support the findings of this study are available from the corresponding author upon reasonable request.

REFERENCES

- ¹K. Samanta and T. S. Dasgupta, *J. Phys. Soc. Jpn.* **87**, 041007 (2018).
- ²R. A. de Groot, F. M. Mueller, P. G. Van Engen, and K. H. J. Buschow, *Phys. Rev. Lett.* **50**, 2024 (1983).
- ³K. W. Lee and W. E. Pickett, *Phys. Rev. B* **77**, 115101 (2008).
- ⁴M. P. Ghimire, L. H. Wu, and X. Hu, *Phys. Rev. B* **93**, 134421 (2016).
- ⁵Y. P. Liu, H. R. Fuh, and Y. K. Wang, *Comput. Mater. Sci.* **92**, 63 (2014).
- ⁶R. Morrow, K. Samanta, T. Saha-Dasgupta, J. Xiong, J. W. Freeland, D. Haskel, and P. M. Woodward, *Chem. Mater.* **28**, 3666 (2016).
- ⁷M. T. Anderson, K. B. Greenwood, G. A. Taylor, and K. R. Poeppelmeier, *Prog. Solid State Chem.* **22**, 197 (1993).
- ⁸S. Vasala and M. Karppinen, *Prog. Solid State Chem.* **43**, 1 (2015).
- ⁹B. Mali, H. S. Nair, T. W. Heitmann, H. Nhalil, D. Antonio, K. Gofryk, S. R. Bhandari, M. P. Ghimire, and S. Elizabeth, *Phys. Rev. B* **102**, 014418 (2020).
- ¹⁰K. K. Wolff, S. Agrestini, A. Tanaka, M. Jansen, and L. H. Tjeng, *Z. Anorg. Allg. Chem.* **643**, 2095 (2017).
- ¹¹M. Arejidal, L. Bahmad, A. Abbasi, and A. Benyoussef, *Physica A* **437**, 375 (2015).
- ¹²A. C. Tian, H. C. Wibowo, Z. Loye, and M. H. Whangbo, *Inorg. Chem.* **50**, 4142 (2011).
- ¹³K. W. Lee and W. E. Pickett, *Phys. Rev. B* **77**, 115101 (2008).
- ¹⁴S. Idrissi, R. Khalladi, S. Mtougui, S. Ziti, H. Labrim, I. El Housni, N. El Mekkaoui, and L. Bahmad, *Physica A* **523**, 714 (2019).
- ¹⁵H. L. Feng, M. Arai, Y. Matsushita, Y. Tsujimoto, Y. Guo, C. I. Sathish, X. Wang, Y. H. Yuan, M. Tanaka, and K. Yamaura, *J. Am. Chem. Soc.* **136**, 3326 (2014).
- ¹⁶H.-S. Lu and G.-Y. Guo, *Phys. Rev. B* **100**, 054443 (2019).
- ¹⁷A. Hossain, P. Bandyopadhyay, and S. Roy, *J. Alloys Compd.* **740**, 414 (2018).
- ¹⁸Y. Yuan, H. L. Feng, M. P. Ghimire, Y. Matsushita, Y. Tsujimoto, J. He, M. Tanaka, Y. Katsuya, and K. Yamaura, *Inorg. Chem.* **54**, 3422 (2015).
- ¹⁹W. Song, E. Zhao, J. Meng, and Z. Wu, *J. Chem. Phys.* **130**, 114707 (2009).
- ²⁰M. El Yadari, L. Bahmad, A. El Kenz, and A. Benyoussef, *J. Alloys Compd.* **579**, 86 (2013).
- ²¹S. Sidi Ahmed, M. Boujnah, L. Bahmad, A. Benyoussef, and A. El Kenz, *Chem. Phys. Lett.* **685**, 191 (2017).
- ²²D. Pesin and L. Balents, *Nat. Phys.* **6**, 376 (2010).
- ²³M. P. Ghimire, R. K. Thapa, D. P. Rai Sandeep, T. P. Sinha, and X. Hu, *J. Appl. Phys.* **117**, 063903 (2015).
- ²⁴B. J. Kim, H. Jin, S. J. Moon, J.-Y. Kim, B.-G. Park, C. S. Leem, J. Yu, T. W. Noh, C. Kim, S.-J. Oh, J.-H. Park, V. Durairaj, G. Cao, and E. Rotenberg, *Phys. Rev. Lett.* **101**, 076402 (2008).
- ²⁵Y. Okada, D. Walkup, H. Lin, C. Dhital, T.-R. Chang, S. Khadka, W. Zhou, H.-T. Jeng, M. Paranjape, A. Bansil, Z. Wang, S. D. Wilson, and V. Madhavan, *Nat. Mater.* **12**, 707 (2013).
- ²⁶X. Wan, A. M. Turner, A. Vishwanath, and S. Y. Savrasov, *Phys. Rev. B* **83**, 205101 (2011).
- ²⁷S. J. Mugavero III, A. H. Fox, M. D. Smith, and H.-C. zur Loye, *J. Solid State Chem.* **183**, 465 (2010).
- ²⁸P. C. Rout and V. Srinivasan, *Phys. Rev. B* **100**, 245136 (2019).
- ²⁹M. P. Ghimire and X. Hu, *Mater. Res. Express* **3**, 106107 (2016).
- ³⁰A. Nid-bahami, A. El Kenz, A. Benyoussef, L. Bahmad, M. Hamedoun, and H. El Moussaoui, *J. Magn. Magn. Mater.* **417**, 258 (2016).
- ³¹R. Morrow, J. R. Soliz, A. J. Hauser, J. C. Gallagher, M. A. Susner, M. D. Sumpston, A. A. Aczel, J. Yan, F. Yang, and P. M. Woodward, *J. Solid State Chem.* **238**, 46 (2016).
- ³²S. R. Bhandari, D. K. Yadav, B. P. Belbase, M. Zeeshan, B. Sadhukhan, D. P. Rai, R. K. Thapa, G. C. Kaphle, and M. P. Ghimire, *RSC Adv.* **10**, 16179 (2020).
- ³³H. P. S. Correa, I. P. Cavalcante, D. O. Souza, E. Z. Santos, M. T. D. Orlando, H. Belich, F. J. Silva, E. F. Medeiro, J. M. Pires, J. L. Passamai, L. G. Martinez, and L. Rossi, *Ceramica* **56**, 193 (2010).
- ³⁴D. Serrate, J. M. D. Teresa, and M. R. Ibarra, *J. Phys.: Condens. Matter* **19**, 023201 (2007).
- ³⁵P. Blaha, K. Schwarz, G. K. H. Madsen, D. Kvasnicka, and J. Luitz, *WIEN2k, An Augmented Plane Wave Plus Local Orbitals Program for Calculating Crystal Properties* (Technische Universität Wien, Vienna, 2001), ISBN: 3-9501031-1-2.
- ³⁶K. Koepf and H. Eschrig, *Phys. Rev. B* **59**, 1743 (1999).
- ³⁷See <https://www.FPLO.de> for detail information about the full-potential local-orbital minimum-basis code.
- ³⁸S. R. Bhandari, R. K. Thapa, and M. P. Ghimire, *J. Nepal Phys. Soc.* **3**, 89 (2015).
- ³⁹M. Rafique, S. Young, and H. Tan, *Physica E* **88**, 115 (2017).
- ⁴⁰J. P. Perdew, K. Burke, and M. Ernzerhof, *Phys. Rev. Lett.* **77**, 3865 (1996).
- ⁴¹A. I. Liechtenstein, V. I. Anisimov, and J. Zaanen, *Phys. Rev. B* **52**, R5467 (1995).
- ⁴²V. I. Anisimov, F. Aryasetiawan, and A. I. Liechtenstein, *J. Phys.: Condens. Matter* **9**, 767 (1997).
- ⁴³C. Kittel, *Introduction to Solid State Physics*, 8th ed. (Wiley, Hoboken, NJ, 2005).
- ⁴⁴D. Serrate, J. M. De Teresa, and M. R. Ibarra, *J. Phys.: Condens. Matter* **19**, 023201 (2007).
- ⁴⁵A. Arulraj, K. Ramesha, J. Gopalkrishna, and C. N. N. Rao, *J. Solid State Chem.* **155**, 233 (2000).
- ⁴⁶N. Zu, R. Li, and R. Ai, *J. Magn. Magn. Mater.* **467**, 145 (2018).
- ⁴⁷H. Kato, T. Okuda, Y. Okimoto, Y. Oikawa, T. Kamiyama, and Y. Tokura, *Phys. Rev. B* **69**, 184412 (2004).
- ⁴⁸Y. Krockenberger, K. Mogare, M. Reehuis, M. Tovar, M. Jansen, G. Vaitheeswaran, V. Kanchana, F. Bultmark, A. Delin, F. Wilhelm, A. Rogalev, A. Winkler, and L. Alff, *Phys. Rev. B* **75**, 020404 (2007).
- ⁴⁹T. K. Mandal, C. Felser, M. Greenblatt, and J. Kubler, *Phys. Rev. B* **78**, 134431 (2008).